Efficacy of cool roofs at reducing pedestrian-level air temperature during projected 21st century heatwaves in Atlanta, Detroit, and Phoenix (USA)

Environmental Research Letters

LETTER

Efficacy of cool roofs at reducing pedestrian-level air temperature during projected 21st century heatwaves in Atlanta, Detroit, and Phoenix (USA)

Ashley M Broadbent[1,2,5], **E Scott Krayenhoff**[1,2,3] **and Matei Georgescu**[1,2,4]

[1] School of Geographical Sciences and Urban Planning, Arizona State University, Tempe, Arizona, United States of America
[2] Urban Climate Research Centre, Arizona State University, United States of America
[3] School of Environmental Sciences, University of Guelph, Guelph, Ontario, Canada
[4] Global Institute of Sustainability, Arizona State University, United States of America
[5] Author to whom any correspondence should be addressed.

E-mail: ashley.broadbent@asu.edu

Keywords: urban climate, heat mitigation, cool roofs, urban expansion, climate change, WRF, cooling effectiveness

Supplementary material for this article is available online

OPEN ACCESS

RECEIVED
15 March 2019

REVISED
9 January 2020

ACCEPTED FOR PUBLICATION
10 January 2020

PUBLISHED
17 July 2020

Abstract

The air temperature cooling impacts of infrastructure-based adaptation measures in expanding urban areas and under changing climatic conditions are not well understood. We present simulations conducted with the Weather Research and Forecasting (WRF) model, coupled to a multi-layer urban model that explicitly resolves pedestrian-level conditions. Our simulations dynamically downscale global climate projections, account for projected urban growth, and examine cooling impacts of extensive cool roof deployment in Atlanta, Detroit, and Phoenix (USA). The simulations focus on heatwave events that are representative of start-, middle-, and end-of-century climatic conditions. Extensive cool roof implementation is projected to cause a maximum city-averaged daytime air temperature cooling of 0.38 °C in Atlanta; 0.42 °C in Detroit; and 0.66 °C in Phoenix. We propose a means for practitioners to estimate the impact of cool roof treatments on pedestrian-level air temperature, for a chosen roof reflectivity, with a new metric called the Albedo Cooling Effectiveness (ACE). The ACE metric reveals that, on average, cool roofs in Phoenix are 11% more effective at lowering pedestrian-level air temperature than in Atlanta, and 30% more effective than in Detroit. Cool roofs remain similarly effective under future heatwaves relative to contemporary heatwaves for Atlanta and Detroit, with some indication of increased effectiveness under future heatwaves for Phoenix. By highlighting the underlying factors that drive cooling effectiveness in a trio of cities located in different climatic regions, we demonstrate a robust framework for estimating the pedestrian-level cooling impacts associated with reflective roofs without the need for computationally demanding simulations.

1. Introduction

Climate projections indicate that the continental United States (CONUS) will be subject to widespread summertime greenhouse gas (GHG) driven warming, on the order of 2 °C–7 °C, by the end of the 21st century (Wuebbles *et al* 2017). Superimposed on GHG-induced climate change are local and regional scale impacts caused by changing land cover characteristics, such as those associated with urbanization. The local climate impact due to urban development can be substantial, depending on urban design characteristics. Maximum nighttime warming resulting from urban expansion in CONUS has been shown to be of similar order of magnitude to GHG-induced warming (Krayenhoff *et al* 2018).

The tendency for cities to be warmer than rural areas, and the associated impacts on energy consumption (Hirano and Fujita 2012, Li *et al* 2012), human health (Stone *et al* 2014, Hondula *et al* 2015), thermal comfort (Wouters *et al* 2017, Broadbent *et al* 2018b), and air quality (Baklanov *et al* 2016, Fallmann *et al* 2016), is a serious challenge urban areas face in

addition to future GHG-induced warming. During heatwave conditions, the adverse impacts of heat can be particularly acute with spikes in human morbidity and mortality (Whitman *et al* 1997, Fouillet *et al* 2006) and electrical grid failures (i.e. 'blackouts') (Lin *et al* 2011, Miller *et al* 2008, McEvoy *et al* 2012) commonly observed. To alleviate extreme urban temperatures, infrastructure-based adaptation measures have been widely proposed and assessed. The spectrum of such strategies includes high albedo surfaces (roofs, roads, and walls) (Li *et al* 2014, Sharma *et al* 2016, Taleghani *et al* 2016), trees and vegetation (Bowler *et al* 2010, Thom *et al* 2016, Vahmani and Ban-Weiss 2016), low thermal admittance construction materials (Krayenhoff *et al* 2018), shade producing architectural features (e.g. narrow streets and shade structures) (Ali-Toudert and Mayer, 2006), as well as water features and irrigation (Daniel *et al* 2018, Broadbent *et al* 2018a). Future urban climates will be determined by dynamic interactions between the regional realization of global climate, the local characteristics of urban growth, and deployment of infrastructure adaptation measures (Georgescu *et al* 2014, Krayenhoff *et al* 2018). Improved understanding of urban adaptation impacts in diverse cities located within distinct climate regimes is required to guide climate adaptation in the developed world and urban planning in the developing world.

We examine the cooling impacts of highly reflective rooftops (i.e. hereafter 'cool roofs') during climatologically representative heatwave conditions. Cool roofs reduce heat load on buildings and decrease the direct conversion of solar energy into sensible heat, providing daytime ambient air temperature cooling. Cool roofs have been widely studied with numerical weather/climate models with reported ambient cooling impacts on the order of 0.1 °C–2 °C (e.g. Oleson *et al* 2010 (global), Fallmann *et al* 2013 (Stuttgart), Schubert and Grossman-Clarke 2013 (Berlin), Huszar *et al* 2014 (Central Europe), Li *et al* 2014 (Baltimore/Washington DC), Ma *et al* 2013 (Beijing), Cao *et al* 2015 (Guangzhou), Salamanca *et al* 2016 (Phoenix), Vahmani *et al* 2016 (Southern California), Zhang *et al* 2016 (global)). The diverse characteristics of cities investigated and lack of standardized practices used when modeling adaptation measures (e.g. intensity of roof albedo change) renders previous findings less helpful to a wider audience. Additionally, regional and global modeling approaches have not resolved the cooling impacts of adaptation measures at pedestrian-level where the cooling impacts are most relevant from a human health and thermal comfort perspective. Further, only a few studies have considered the impacts of cool roofs under changing climate and future urban growth scenarios to examine their effectiveness across varying geographies and time periods (Georgescu *et al* 2012, 2013, 2014, Krayenhoff *et al* 2018). Such studies have typically used medium spatial resolutions (e.g. 20 km) to assess seasonally averaged impacts of cool roof deployment and do not capture the local-scale intra-urban air temperature variability, driven by differences in urban morphology (i.e. roof area, building height and spacing), commonly observed in cities (Stewart and Oke 2012). We build on this previous work by conducting high-resolution numerical simulations (1 km grid spacing) to simultaneously investigate the impacts of urban growth, cool roof deployment, and global climate change for a trio of US cities located across distinct geographies: Atlanta, Detroit and Phoenix. The cities have broadly contrasting ecological characteristics (i.e. vegetation type and presence of water bodies), building morphologies, and projected rates of urban growth.

Urban planners and policy makers may ask the following question: how much cooling will cool roof implementation provide in our city and/or neighborhood? The answer to this question is determined by the local building morphology, the intensity of cool roof implementation, the average albedo of pre-existing roofs, and the climatic characteristics of the city. The absolute cooling impacts of cool roofs have been simulated in many cities, but their findings are not reported in a generalizable way and are therefore of reduced utility for planners and practitioners outside the city of interest. Despite this lack of guidance, municipalities are already experimenting with and implementing cooling infrastructure at scale (e.g. cool roof and cool pavement initiatives in Los Angeles, CA). Consequently, there is a need for robust and generalizable metrics that are suitable for estimating the cooling impacts of adaptation measures in different cities/neighborhoods prior to their deployment.

We seek to address the following research questions:

(1) What are the absolute ambient pedestrian-level air temperature impacts of intensive implementation of cool roofs in Atlanta, Detroit, and Phoenix during climatologically representative heatwaves for contemporary, mid-, and end-of-century time periods?

(2) Across which urban landscapes and in which time periods are commercially available cool roofing materials most effective (i.e. provide the most cooling per unit of roof changed) and what drives differences in cooling effectiveness?

(3) Can cool roofs offset the broad impacts of urban expansion and GHG-induced heatwave intensification?

2. Methods

2.1. Heatwave identification

We simulate representative heatwaves for each city that are characteristic of three 30 year time periods:

start-century (1981–2010), mid-century (2041–2070), and end-of-century (2071–2100). We identify heatwave events from each time slice using historical observations (airport weather stations from the Global Historical Climate Network, GHCN) and Community Earth System Model (CESM) CMIP5 projections for regional concentration pathway (RCP) 4.5 and 8.5. We identify extreme heatwave events that have a climatologically consistent relative intensity across RCPs/time periods. Our heatwave identification approach prioritizes inter-comparability of heatwaves across all cities and time periods. The case study heatwaves selected are among the most extreme events (i.e. the top decile of 5 d heatwaves) projected to occur during each 30 year time period and are likely to be associated with temperatures that cause increased human mortality and morbidity (see table S1 for heatwave details). For consistency, our analysis focuses on the five hottest consecutive days within each heatwave as defined by our process-based modeling tool (see section 2.2) after dynamical downscaling (hereafter this period is referred to as 'HW5'). Additional information on heatwave identification is provided in Supplementary Methods (section S1.1 or figure S1 is available online at stacks.iop.org/ERL/15/084007/mmedia).

2.2. WRF model setup

We conduct all simulations with the Advanced Research (ARW) version of the WRF regional climate model (v3.6.1) (Skamarock and Klemp 2008). The lateral boundary conditions (i.e. the WRF meteorological context) for contemporary simulations are obtained from the ERA-Interim reanalysis (European Centre for Medium-Range Weather Forecasts ECMWF ERA-Interim Project 2009). For future simulations, we use the mid and end-of-century bias-corrected output from CESM CMIP5 ensemble member six, for RCP 4.5 and 8.5 model integrations (Monaghan *et al* 2014). RCP 8.5 assumes continued population growth and GHG emissions with minimal climate change mitigation policies enacted. RCP 4.5 represents implementation of climate policies and reduced emissions, stabilizing future temperatures by the end of the 21st century.

WRF simulations center on heatwave periods that are representative of each city/time period and emissions scenario: start-century ERA-Interim (hereafter 'START'), mid-century CESM RCP 8.5 (hereafter 'MID85'), end-of-century CESM RCP 4.5 (hereafter 'END45'), and end-of-century CESM RCP 8.5 (hereafter 'END85'). Mid-century RCP 4.5 heatwaves will not substantially differ from mid-century CESM RCP 8.5 conditions and given the computational cost associated with such simulations, we decided not to simulate mid-century RCP 4.5 conditions.

Our model setup has three nested domains for all WRF simulations with horizontal grid spacing of 16, 4, and 1 km (impervious fraction of the inner model domain for each time period/city is shown in figures 1 and S2 (RCP 4.5 only)). For the vertical grid, we define 42 levels with the finest grid spacing (i.e. $<$3 m) at the surface. Critically, the lowest level is located between the buildings within the urban canopy at approximately 2 m height above the ground, ensuring urban pedestrian-level air temperature is captured. By contrast, urban temperatures derived from the commonly used single-layer urban canopy model are not representative of the 2 m level, but are instead diagnosed based on heat flux from the complete urban surface (including rooftops). We therefore expect our approach to provide more realistic street-level cooling estimates than commonly used single layer approaches, which is critical for understanding the human thermal comfort and health implications of adaptation. See table S2 for a full summary of WRF physics schemes used in this analysis.

Urban areas are modeled by the Building Environment Parameterization (BEP) (Martilli *et al* 2002). To define contemporary and future urban land cover we use the US Environmental Protection Agency's (EPA) Integrated Climate and Land-Use Scenarios Version 2 (ICLUSv2) (Bierwagen *et al* 2010, U.S. EPA 2017). ICLUSv2 projects RCP-specific human population, land-use, housing density, and impervious surfaces across the US. The building morphological characteristics represented in BEP include roof area, building height and spacing (see table S3). For all simulations, we match the urban growth scenario with the future climate conditions; thus, we have simultaneously accounted for the impacts of urbanization and GHG-induced climate change in our simulations (see details in section S1.2).

Cool roofs are represented by uniformly increasing the roof surface albedo of all rooftops from 0.16 to 0.88. The reflectivity of high albedo roof coatings may degrade due to weatherization and soiling associated with dust and black carbon deposits and biomass accumulation, with average reported decreases in albedo of up to 0.2 (Levinson *et al* 2005, Ferrari *et al* 2014). We assume a near maximum sustained roof albedo (0.88) obtained from a 'SOLARFLECT' coating after three years of wear and tear according to the EPA Energy Star roof product list (https://downloads.energystar.gov/bi/qplist/roofs_prod_list.pdf?8ddd-02cf). Therefore, the ambient cooling reported here represents near maximum impacts associated with existing commercially available cool roofing materials.

2.3. Model evaluation

We evaluate WRF performance against available near surface weather stations and upper air soundings. We obtained weather station data from GHCN, Arizona

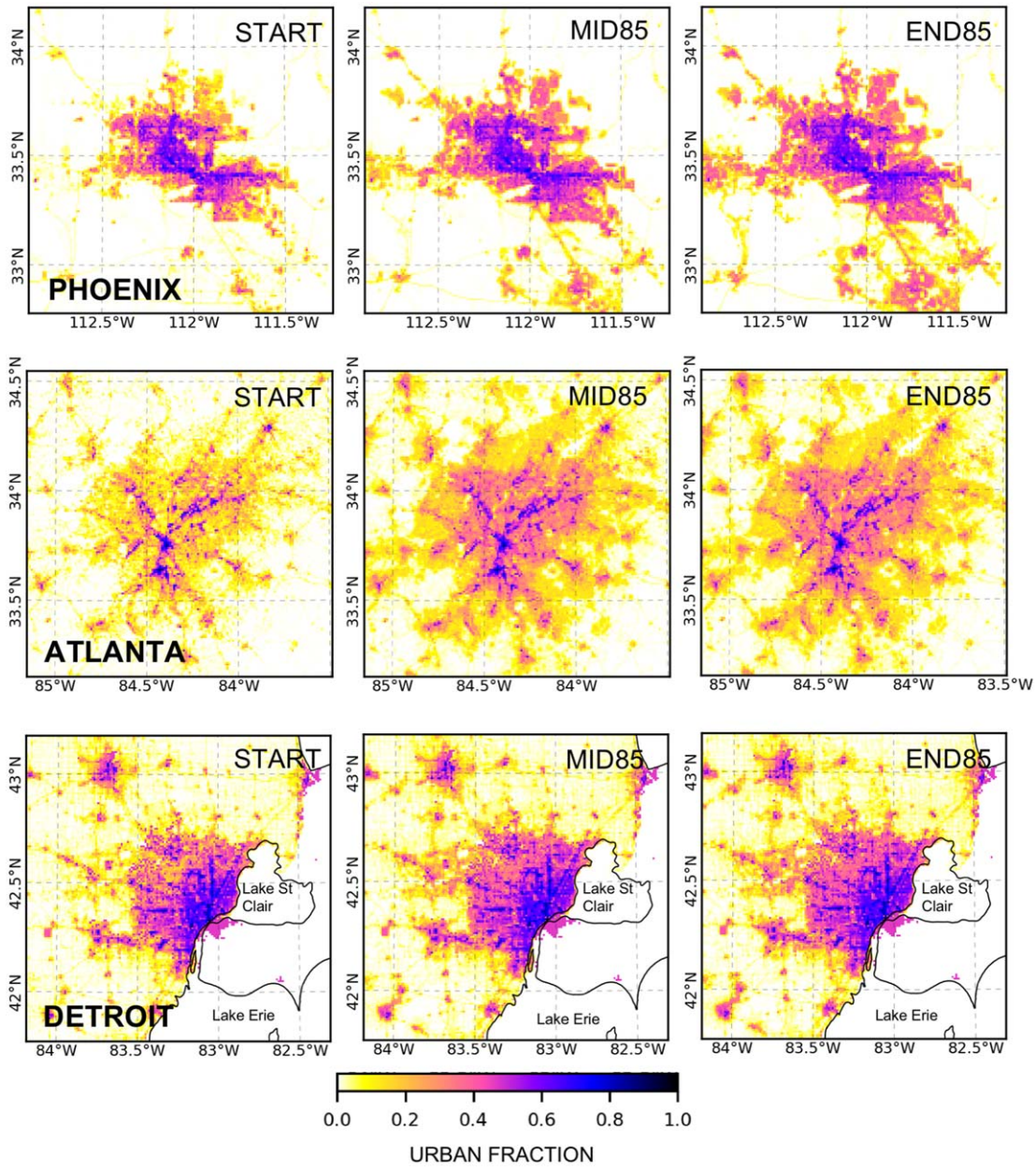

Figure 1. Representation of impervious fraction for inner-most WRF domains (1 km by 1 km grid spacing) for Phoenix (top row), Atlanta (middle row), and Detroit (bottom row). Three time periods/RCP scenarios (shown left to right) are shown: START = start-century, MID85 = mid-century RCP 8.5, and END85 = end-century RCP 8.5. For end-century RCP 4.5 imperviousness, see figure S2. For the Detroit panels, the outline of lakes in the domain are shown (see figure S3 for more detail).

Meteorological Network (AZMET) (https://cals.arizona.edu/azmet/), MesoWest (https://mesowest.utah.edu/), the Maricopa County Air Quality Department (https://maricopa.gov/1643/Air-Quality-Status-and-Monitoring), and sounding data from the National Weather Service (NWS) (obtained via University of Wyoming website: http://weather.uwyo.edu/upperair/sounding.html). Overall, we find that timing and amplitude of surface air temperatures are satisfactorily captured in all three cities, and we report that the evolution of urban boundary layer (UBL) thermal structure is broadly reproduced (see supplementary results, section S2.1 for details).

3. Results

3.1. Intensity of projected heatwaves

Simulation results show that WRF-simulated future heatwave intensity will increase in all three cities (table 1). Atlanta and Detroit will experience 4 °C–5 °C increases in both average daily maximum and minimum temperatures during high intensity end of the century heatwaves. Phoenix, which is already situated in a very hot and dry climate, is projected to experience a smaller increase in high intensity heatwave temperatures than Detroit and Atlanta with 1.8 °C and 0.6 °C increases in average daily maximum and minimum temperatures, respectively.

Table 1. WRF-simulated air temperatures during the 5 hottest consecutive days of the heatwave (HW5). We used the median value of all urban grid squares to calculate the values below.

	Diurnal (°C)			
City	START	MID85	END45	END85
Phoenix	38.8	39.6	39.6	40.6
Atlanta	30.1	33.0	31.9	34.4
Detroit	28.3	30.2	29.9	33.1
	Maximum (°C)			
Phoenix	45.5	47.3	47.3	48.3
Atlanta	35.4	38.6	37.6	40.1
Detroit	34.1	34.1	35.3	38.2
	Minimum (°C)			
Phoenix	31.7	31.7	31.2	32.3
Atlanta	24.6	27.9	25.8	28.8
Detroit	22.3	26.3	23.8	27.5

3.2. Absolute cooling impacts of cool roofs

Across all cities and time periods, cool roofs predominantly provide daytime cooling of pedestrian-level air temperature and minimal nighttime cooling (see panels in figures 2 and S8 (RCP 4.5 only)). Nighttime cooling impacts are negligible for Atlanta and Detroit, while a small (up to −0.29 °C) but significant nighttime impact is simulated for Phoenix. As most of the cooling is projected during the day, we primarily focus on the daytime effects of cool roofs throughout this analysis.

The average change in daytime 2 m air temperature, hereafter (ΔT_{day}), during HW5 for urban grid squares, due to city-wide implementation of cool roofs in Phoenix ranges from −0.45 °C during the START simulation to −0.66 °C for the END85 simulation. In Atlanta, the ΔT_{day} is predicted to range between −0.11 °C (START) and −0.38 °C (END45). The ΔT_{day} in Detroit is consistent across the four time periods, falling between values of −0.35 °C (START) and −0.42 °C (END45). Daily maximum temperature change (averaged from 11 am through 2 pm local time) reaches −2.5 °C in Phoenix and −2.0 °C in Atlanta and Detroit (see daily maximum cooling in figure S9). Overall, Phoenix is characterized by the largest average and daily maximum pedestrian-level air temperature cooling impacts from widespread cool roof deployment.

There is also spatial variability of daytime cooling from cool roofs, demonstrating the pedestrian-level cooling impacts are non-uniform across a city (figures 3 and S10 (END45 only)). High (cool) roof area is the primary cause of air temperature cooling spatial maxima; however, other factors influence intra- and inter-urban variability in cooling impacts from cool roofs. It is important for practitioners to understand where cool roof deployment could provide the most pedestrian cooling. In the subsequent sections, we focus on the concept of cooling effectiveness. We ask: where will cool roofs provide the most pedestrian-level cooling per unit of rooftop modified?

3.3. Cooling effectiveness

Cooling effectiveness can be thought of as the average ΔT_{day} resulting from a given change in albedo ($\Delta\alpha$) for a specific city/time period combination. One metric of cooling effectiveness is a regression model of total surface $\Delta\alpha$, due to conversion of conventional to cool roofs, against HW5 ΔT_{day} (see figure 4, left panels). A higher $\Delta\alpha$ represents a more intense application of cool roofing materials. The regression models are non-linear for Atlanta and Detroit, but in Phoenix approximate linearity in 2 of 4 cases (e.g. MID85 and END45). Further, a regression model derived from a composite of all 4 Phoenix simulations is in fact linear (see figure S11), indicating the pedestrian cooling impacts of cool roofs remain approximately constant across the range of $\Delta\alpha$ values examined for Phoenix. The shape and slope of the curves imply cool roofs in Phoenix will provide more cooling per unit albedo change compared to the other cities.

However, treating all grid squares in the domain as a single population and fitting a regression model partially obscures the spatial variability in these data. To investigate this variability, we introduce a second metric of cooling effectiveness following Krayenhoff and Voogt (2010). The albedo cooling effectiveness (ACE) for each urban grid square is calculated as:

$$ACE = \Delta T_{day}/\Delta\alpha, \quad (1)$$

where $\Delta\alpha$ refers to plan area average albedo change (due to cool roofs), and a negative ACE indicates greater cooling effectiveness. ACE exhibits complex spatial patterns (see figures 5 and S12 (RCP 8.5 only)), the drivers of which are addressed in subsequent sections. Across all urban densities and time periods (see black boxplots in figure 4, right), Phoenix has the highest average ACE of −6.50 °C, followed by Atlanta with −5.85 °C, and finally Detroit has the lowest ACE of −4.78 °C. The average differences between city ACE values are statistically significant for all cities at the 0.01 significance-level (Welch's t-test). Phoenix also exhibits an increasingly negative ACE between START and END85 simulations, which implies an increasing effectiveness of cool roofs under future climate and urbanization. A trend of increasing cooling effectiveness between START and END85 heatwaves was not apparent for both Atlanta and Detroit. Overall, ACE values imply that, across all urban densities and time periods, cool roofs in Phoenix are 11% more effective at cooling pedestrian-level air temperature than in Atlanta, and 30% more effective than in Detroit.

3.4. Impacts of building morphology on cooling effectiveness

The morphology of buildings, specifically the height and density, directly impact the cooling effectiveness of cool roofs. Cool roofs are more effective in low-density areas than medium and high-density urban areas by factors of 1.8 or more (figure 4–i.e. Detroit mean low density ACE = 6.5 and mean medium/high

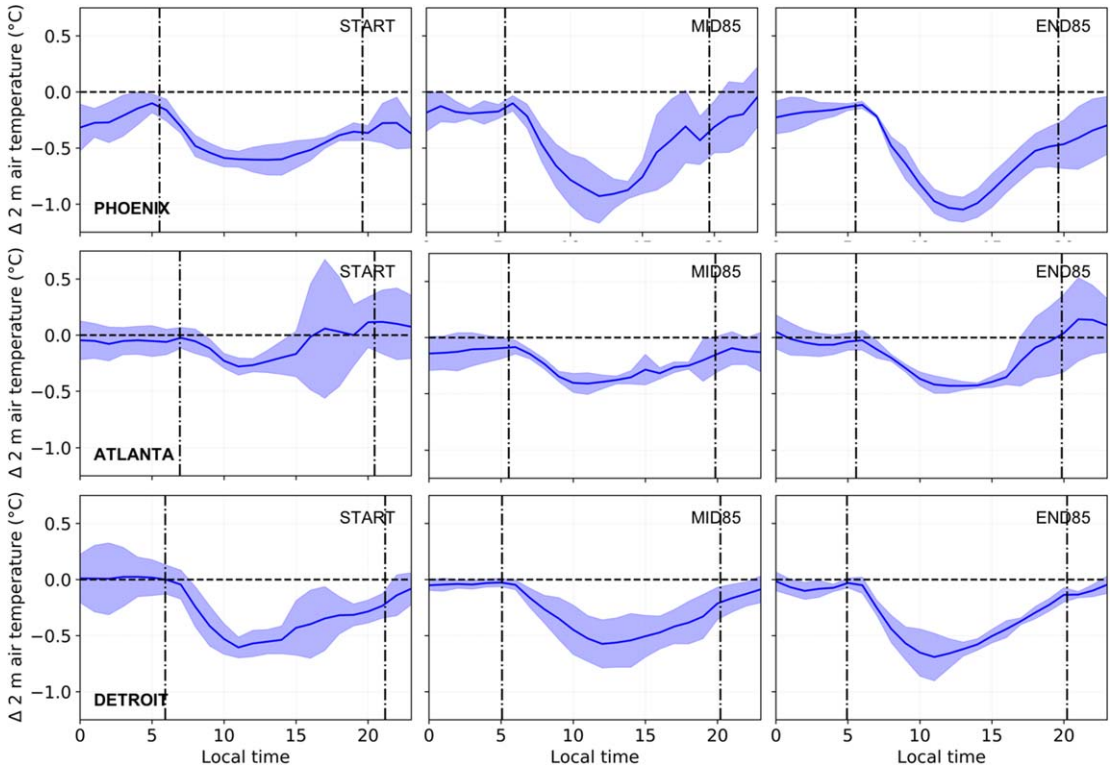

Figure 2. Composite diurnal averages of the mean change in WRF simulated 2 m air temperature for each urban area during the 5 hottest consecutive days of heatwave (HW5) due to implementation of cool roofs for Phoenix (top row), Atlanta (middle row), and Detroit (bottom row). Vertical lines show sunrise and sunset in local time and shaded areas represent one standard deviation about the mean. Three time periods/RCP scenarios are shown; START = start-century, MID85 = mid-century RCP 8.5, and END85 = end-of-century RCP 8.5. Cool roofs are represented by increasing the rooftop albedo of all roofs in WRF from 0.16 to 0.88.

density ACE = 3.7). The cooler air at roof-level can be efficiently mixed towards street-level when buildings are short (i.e. single story) and building plan area is low (i.e. 0.33 or lower). Our approach explicitly resolves this mixing via application of the multi-layer BEP model with very high vertical resolution within the urban canopy layer. Higher cooling effectiveness in low-density urban areas holds even when grid squares with the same total albedo change are compared. Figure S13 shows that low-density urban areas with $\Delta\alpha < 0.10$ receive more cooling than medium- and high-density areas with $\Delta\alpha < 0.10$ (i.e. the same albedo change), suggesting that building morphology and not some other factor (e.g. advection) is the primary cause of higher effectiveness in the lowest-density urban areas.

We postulate that transport of lower temperature air from cool roofs would increase cooling effectiveness in areas downwind of the heavily built-up areas. Therefore, horizontal transport (i.e. advection) of cool air from cool roofs may disproportionately impact low-density suburban areas, which are more commonly located on the urban fringes. However, Atlanta and Detroit exhibit no clear gradients of ACE along the axis of prevailing wind (see figure 5 middle and bottom rows). In Phoenix, higher cooling ACE values in the north-east (downwind) are apparent compared to the south-west (upwind) of the city. The cooling effectiveness in low-density areas is about 25% greater on the north-east side of Phoenix relative to the south-west (the dashed line in figure 5 shows the cutoff used). This gradient indicates that low-density urban grid squares on the north-eastern side of Phoenix may be receiving an enhanced non-local advective cooling benefit, resulting in a greater apparent cooling effectiveness in those areas.

3.5. Surface energy balance drivers of cooling effectiveness

Inter-urban differences in surface energy balance derived from cool roof deployment explain the impacts of distinct climatologies and surface energy balance characteristics on cool roof cooling effectiveness. The relationship between the change in surface fluxes and $\Delta\alpha$ (see figure 6) reveal how cool roofs modify the urban surface energy balance in each city. Since cool roofs reduce absorbed solar radiation, the modification of absorbed shortwave radiation (ΔK^*) is the principal agent that ultimately drives air temperature cooling. The primary cause of inter-city differences in the magnitude of ΔK^* during heatwave conditions is latitude. In Phoenix and Atlanta, the relationship between ΔK^* and $\Delta\alpha$ is indistinguishable, which is commensurate with their similar latitudinal locations in the US Sunbelt (figure 6(b)). Thus, deployment of cool roofs will generally be more effective at cooling 2 m

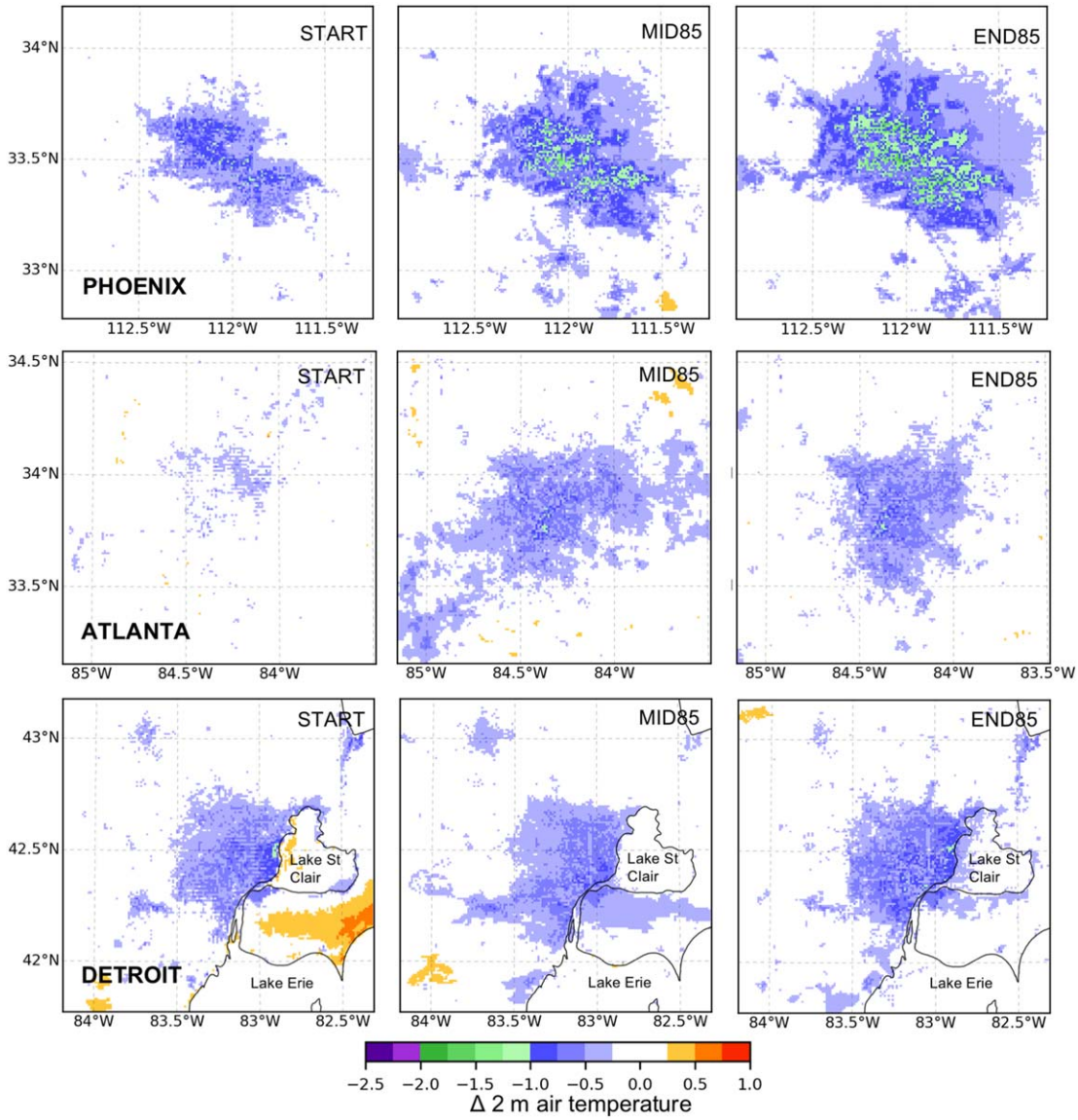

Figure 3. WRF-simulated change in daytime 2 m air temperature (ΔT_{day}) during the 5 hottest consecutive days of heatwave (HW5) due to implementation of cool roofs for Phoenix (top row), Atlanta (middle row), and Detroit (bottom row). Cool roofs are represented by increasing the rooftop albedo of all roofs in WRF to 0.88. Three time periods/RCP scenarios are shown here; START = start-century, MID85 = mid-century RCP 8.5, and END85 = end-of-century RCP 8.5. For the Detroit panels, the outline of lakes in the domain are shown.

air temperature in the Sunbelt than the Midwest and northern regions of the US.

Clouds also impacted cooling effectiveness in Atlanta and Detroit by intermittently intercepting downwelling shortwave radiation ($K\downarrow$) (table S4). Cities with less cloud coverage (e.g. Phoenix) are likely to receive more effective cooling outcomes from cool roofs; the difference in effectiveness of cool roofs between Phoenix and other cities will be even larger on a summertime average basis, when impacts of clouds are more pronounced based on large-scale climate differences (e.g. see Krayenhoff *et al* 2018).

In addition to the impacts of clouds and latitude, the characteristics of the surface energy balance, likely driven by differences in local vegetation and moisture, appear to impact the effectiveness of cool roofs. Atlanta and Detroit have more surface moisture availability than Phoenix due to the presence of evapotranspiring vegetation (Atlanta) and water bodies (Detroit). We identify three surface energy balance processes that stand out in Phoenix and contribute to more effective cooling outcomes: (1) in drier environments with less evapotranspiring vegetation or water bodies, cool roofs appear to cause a larger reduction in surface-to-atmosphere heat exchange via sensible heat flux (ΔQ_H); (2) cool roofs drive more heat dissipation through longwave emission ($L\uparrow$) in Phoenix than in Atlanta and Detroit; and (3) cool roofs lead to the greatest diversion of energy from heat storage (Q_G) in Phoenix; likely contributing to the small nighttime cooling effect observed there. A more detailed description of these factors is provided in the Supplementary Results (section S2.3).

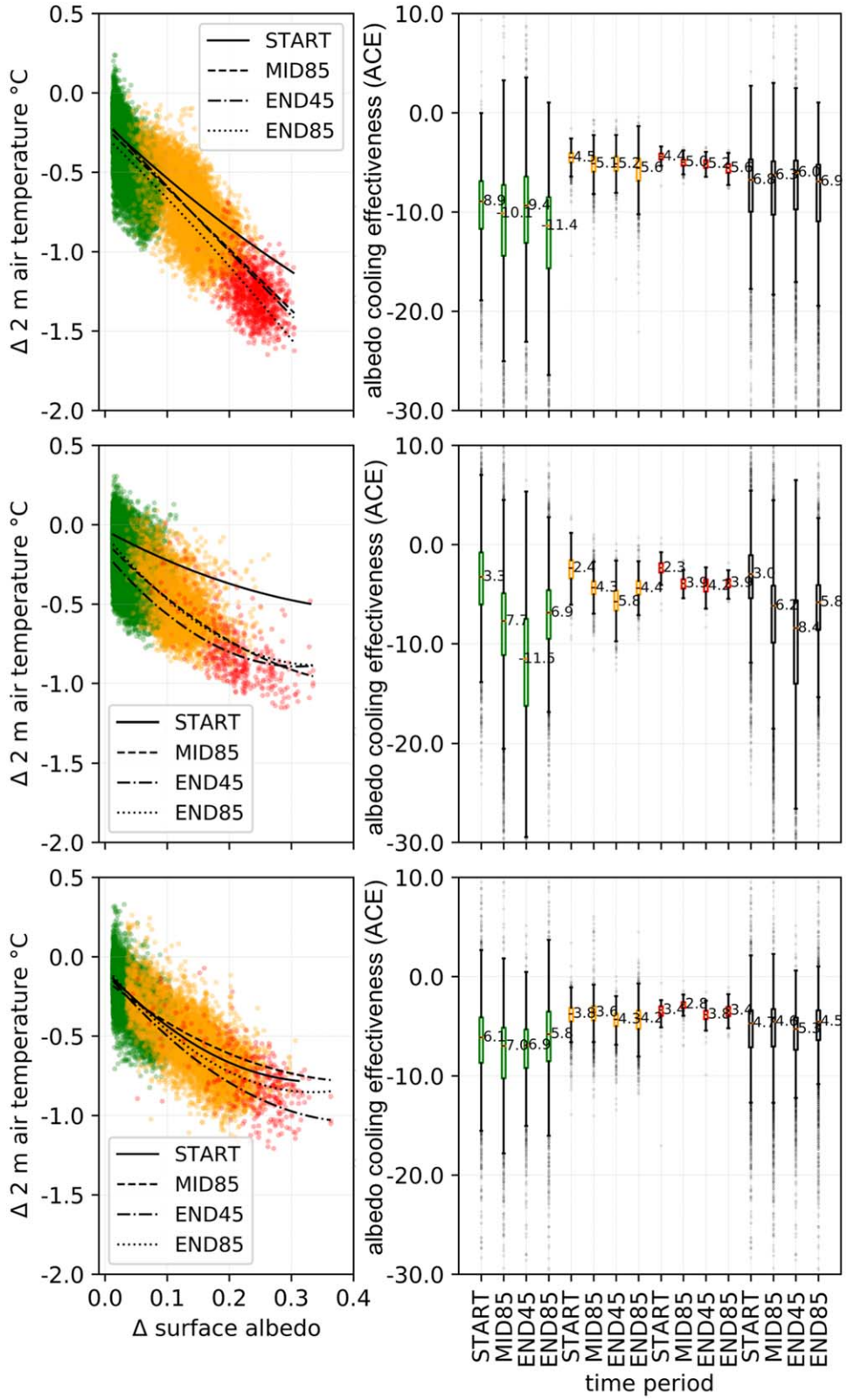

Figure 4. WRF simulated cooling effectiveness of cool roofs for daytime hours during the five hottest consecutive days of each heatwave (HW5). The scatter plots (left) show the change of plan area average surface albedo ($\Delta\alpha$) versus change in daytime air temperature (ΔT_{day}) for all simulations, grouped by city. A best-fit representation for each time period is shown; see legend in each left-hand column panel. Boxplots (right) show the distributions of daytime albedo cooling effectiveness (ACE) for each urban land cover category (color-coded) and time period. The dots and boxes are color-coded: green = low density urban, orange = medium density urban, red = high density urban, and black (boxes only) = all urban grid squares. START = start-century, MID85 = mid-century RCP 8.5, END45 = end-of-century RCP 4.5, and END85 = end-of-century RCP 8.5.

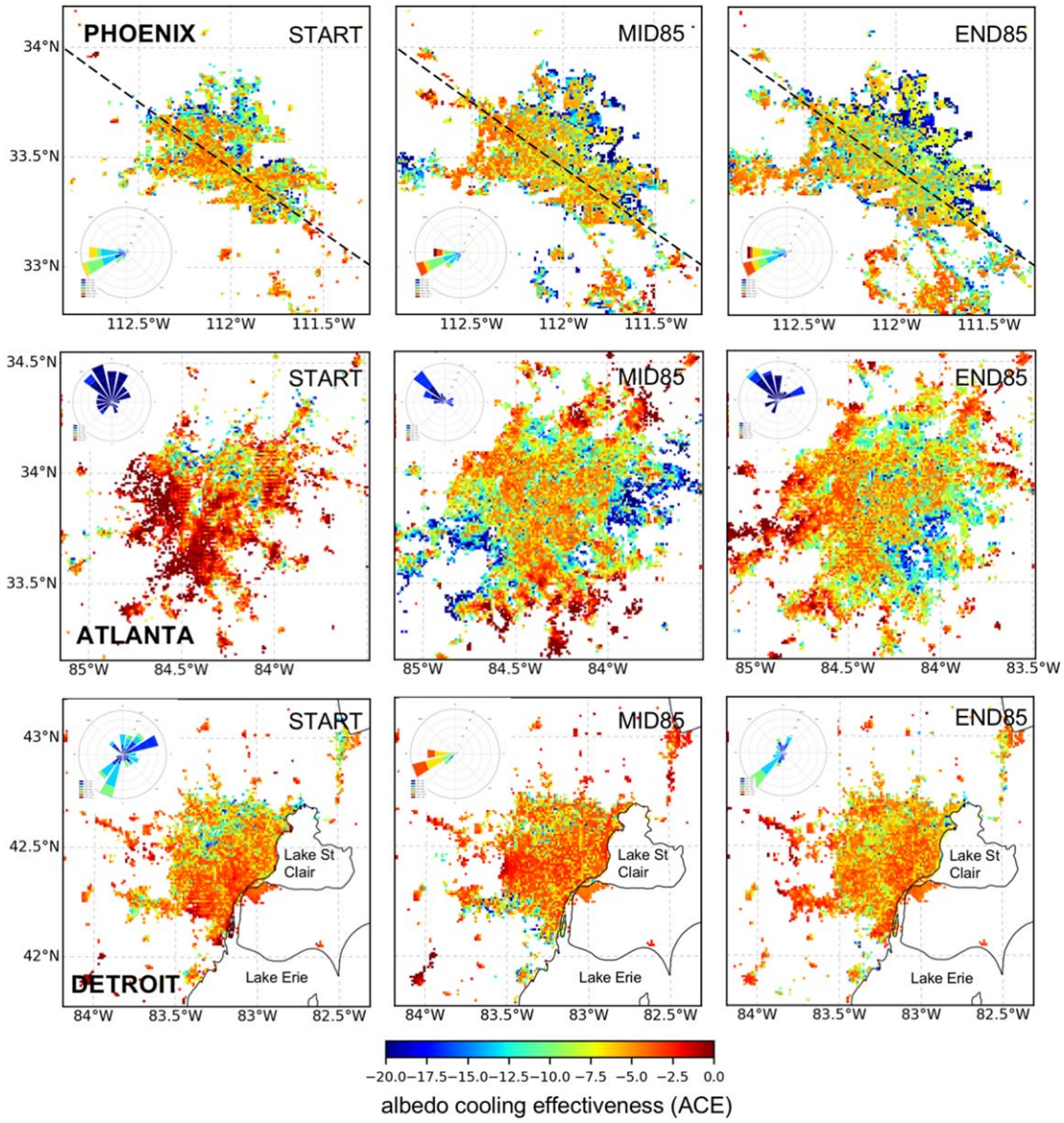

Figure 5. WRF-simulated daytime albedo cooling effectiveness (ACE) during the 5 hottest consecutive days of heatwave (HW5) due to implementation of cool roofs in Phoenix (top row), Atlanta (middle row), and Detroit (bottom row). Cool roofs are represented by increasing the rooftop albedo of all roofs in WRF to 0.88. Three time periods/RCP scenarios are shown; START = start-century, MID85 = mid-century RCP 8.5, and END85 = end-of-century RCP 8.5. Wind roses in insets show the wind speed and direction during the HW5. Dashed line in top row indicates cut-off used for advection impact calculations (see section 3.4).

3.6. Offsetting GHG and urbanization warming impacts with cool roofs

Another key question for practitioners is to what extent cool roofs can offset the increased intensity of future heatwaves due to GHG warming and urbanization. To address this question, we calculate the following metric for each WRF grid square:

$$\Delta T_{OFFSET} = T_{START} - T_{FUTURE}, \quad (2)$$

where T_{START} is daytime air temperature for the start-century heatwave without cool roofs and T_{FUTURE} is the daytime air temperature in a future heatwave (i.e. MID85, END45, or END85) with city-wide deployment of cool roofs implemented. $\Delta T_{OFFSET} > 0$ does not indicate that cool roofs are ineffective, but rather that the cooling impact of cool roofs is smaller than the combined effects of GHG and urbanization induced warming.

Full deployment of cool roofs in Phoenix nearly offsets GHG and urban-induced warming, resulting in a HW5 ΔT_{OFFSET} of 0.14 °C (MID85), 0.36 °C (END45), and 0.71 °C (END85) (see figures 7 and S14 (RCP 4.5 only)). Atlanta probability distributions of HW5 ΔT_{OFFSET} have the narrowest range of values, generally falling in a 2 °C window (figures 7(c) and (d)). Cool roofs shift the distribution to the left for Atlanta, but the median HW5 ΔT_{OFFSET} still increase by 2.65 °C (MID85), 1.39 °C (END45), and 3.95 °C (END85), indicating that cool roofs fall short of offsetting future GHG and urban induced warming in this city. Finally, the largest range of ΔT_{OFFSET} is simulated for Detroit (figures 7(e) and (f)), although cool roofs cannot offset GHG and urban induced future warming; HW5 median ΔT_{OFFSET} values of 0.96 °C

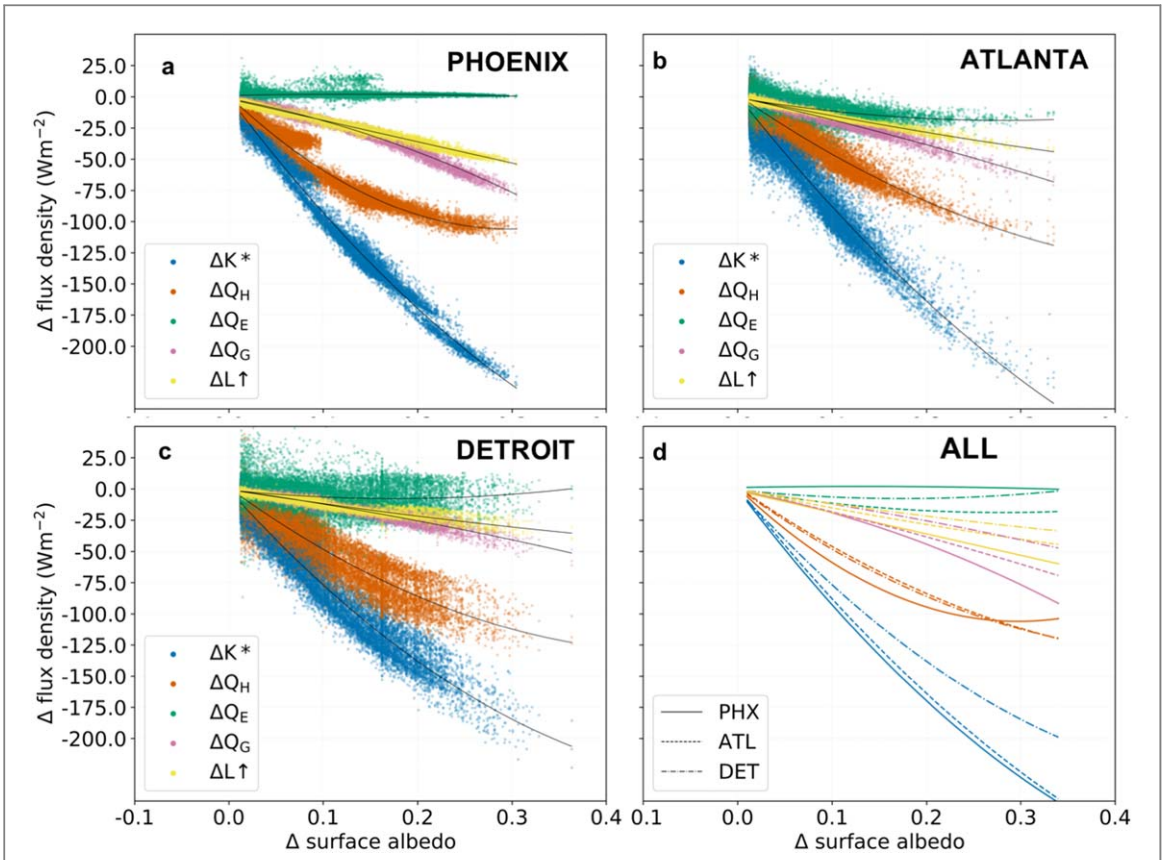

Figure 6. WRF-simulated mean daytime change in energy balance fluxes due to cool roof implementation plotted against change in plan area average surface albedo change during the 5 hottest consecutive days of the heatwave (HW5) for (a) Phoenix, (b) Atlanta, (c) Detroit. Panels (a)–(c) contain results from four simulations (dots) with polynomial regression models fitted through all four simulations. Panel (d) contains the same regression models from (a)–(c) overlain for comparison purposes. K^* = net shortwave radiation, Q_H = sensible heat flux, Q_E = latent heat flux, Q_G = ground heat flux, and $L\uparrow$ = emitted longwave radiation.

(MID85), 0.86 °C (END45), and 3.63 °C (END85) are projected for Detroit.

Our analysis incorporates climate forcings from a single GCM (CESM CMIP5 ensemble member six) and we do not account for the full range of uncertainty in future climate by including additional GCM forcings. The CESM forcing represents the CMIP5 median for projected end-of-century summertime CONUS temperatures. Therefore, the impacts of cool roofs relative to GHG induced warming should be appropriately interpreted in light of this constraint.

4. Discussion and conclusions

This work advances scientific understanding on the effectiveness of reflective roofing materials to provide pedestrian-level air temperature cooling in expanding urban areas and under changing climatic conditions. Our high-resolution simulations (i.e. 1 km) simultaneously account for projected GHG-induced climate change and urban expansion across a trio-of US cities located in differing climatic zones. We incorporate newly developed projections of US urban land cover (ICLUS Version 2) to represent urban expansion at high spatial resolution. Unlike previous work, our analysis does not merely investigate absolute air temperature changes resulting from adaptation measures; we introduce and develop a new metric of cooling effectiveness (ACE) that allows practitioners to assess the street-level cooling impacts of cool roofs based on knowledge of building density and roof albedo change (i.e. easily attainable data). This metric also provides a framework for standardized reporting of adaptation cooling impacts that should be adopted by the climate community to ensure consistent reporting that can be meaningfully interpreted by professionals in the field. Finally, we conduct a novel assessment of how cool roofs modify the urban surface energy balance across different neighborhoods and climatic zones, highlighting the potential for a metric such as ACE to be used across cities with similar characteristics.

Our findings have important implications for planners, developers, and policy-makers seeking to implement cool roofs in existing or emerging urban environments. We demonstrate the variable effectiveness of cooling associated with cool roofs both between and within cities, and provide insights to practitioners seeking to strategically implement cool roofs in a targeted and effective fashion. Specifically, we have developed a metric of cooling effectiveness (i.e. ACE); the average neighborhood cooling from cool roofs can be estimated as:

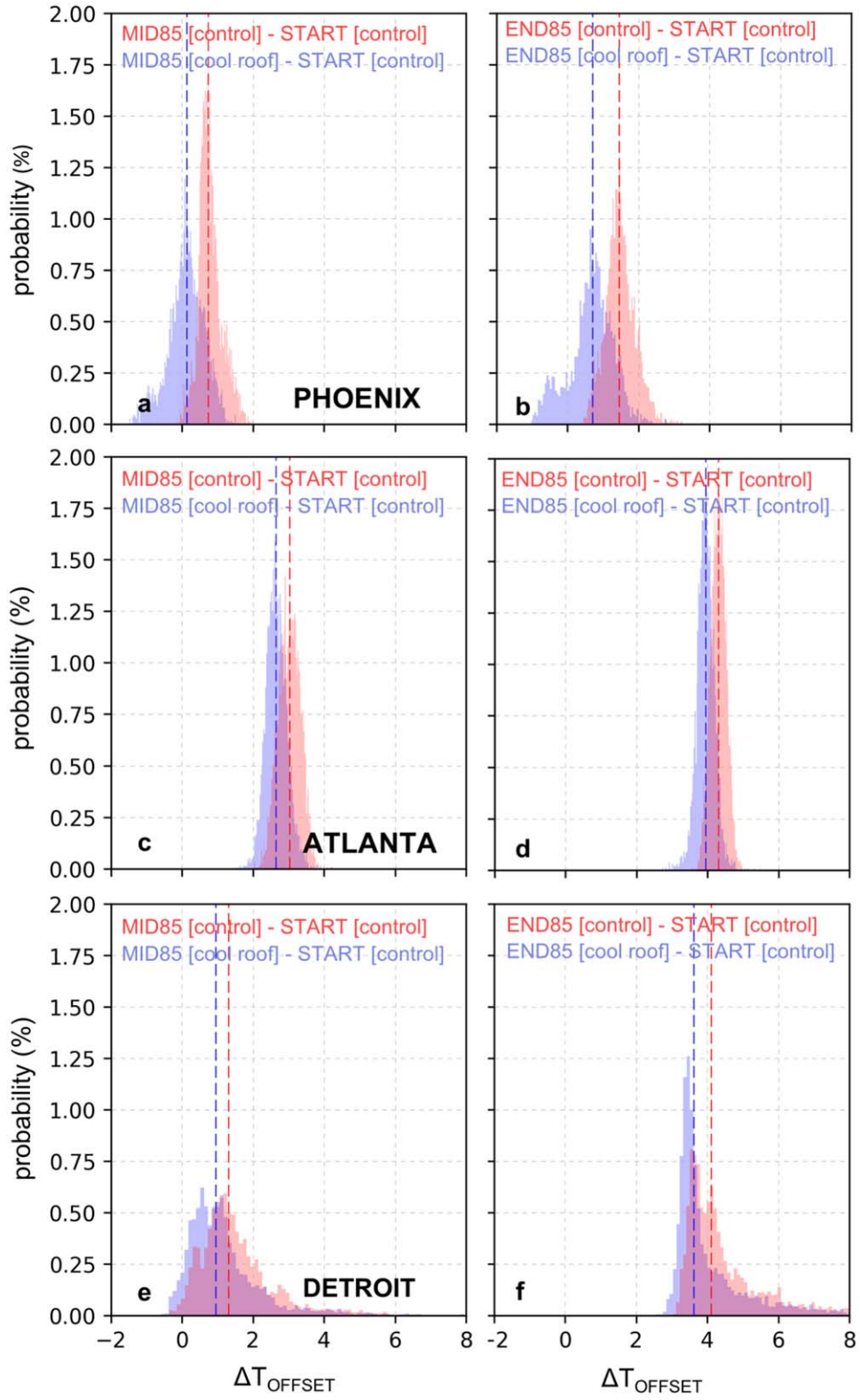

Figure 7. Probability density functions of WRF-simulated mean difference in daytime 2 m air temperature between START and a future simulation (ΔT_{OFFSET}) for the 5 hottest consecutive days of heatwave (HW5). The future simulations are: MID85 (left column) and END85 (right column) for Phoenix (top row), Atlanta (middle row), and Detroit (bottom row). Dashed vertical lines indicate the median of each distribution. START = start-century, MID85 = mid-century RCP 8.5, and END85 = end-of-century RCP 8.5.

$$\Delta T = \Delta\alpha_{ROOF} \times \lambda_{ROOF} \times ACE, \quad (3)$$

where $\Delta\alpha_{ROOF}$ is average change in roof albedo due to cool roofs, λ_{ROOF} is the plan area of roofs receiving albedo treatment (i.e. roof area divided by total ground area in the neighbourhood), and ACE depends on geographic location, season, and building density. In cases where λ_{ROOF} and $\Delta\alpha_{ROOF}$ are unknown, a practitioner can use representative values associated with Local Climate Zones (LCZ) (see Stewart *et al* 2014). For example, to calculate the cooling impacts of a proposed 0.85 roof albedo

treatment in an open-low-rise (LCZ 6) neighborhood, one can assume $\lambda_{ROOF} = 0.30$, $\alpha_{ROOF} = 0.13$, and $\Delta\alpha_{ROOF} = 0.85–0.13 = 0.72$. Additionally, the ACE metric may also be used to estimate the diminishing cooling impacts of cool roofs due to weatherization and soiling by simply reducing the $\Delta\alpha_{ROOF}$ term in equation 3.

Based on our analysis of surface energy balance, we hypothesize that the key drivers of variability in ACE are building morphology (height and density), latitude, cloud cover, and local surface energy balance characteristics. Therefore, we believe that our results are most generalizable across cities that are comparable to Detroit, Atlanta, and Phoenix. At the city planning level, a key implication of this research is that cool roofs may be more effective at providing heatwave cooling in the US Sunbelt than in the Midwest. Rapidly growing Sunbelt cities (e.g. Los Angeles, Las Vegas, Dallas, Houston, Atlanta, Tampa, and Phoenix) can expect greater cooling per unit of cool roof implemented during heatwaves than northern and Midwest cities. In addition, the increased effectiveness of cool roofs is likely to be enhanced in drier cities in the western Sunbelt, primarily due to less cloud formation than the eastern Sunbelt.

Our analysis focuses on the cooling impacts of a single technology (cool roofs), in three different cities, during heatwave conditions. We acknowledge that cool roofs are but one heat adaptation strategy amongst many that practitioners may choose to adopt. Nevertheless, our analysis is a useful way to systematically assess the adaptation potential and cooling impacts of cool roofs, which are among the most commonly proposed adaptation measures. Our analysis, including surface energy balance and air temperature, concludes that estimates of cooling effectiveness could be broadly applied across different cities with similar latitudinal locations, climatologies, and urban morphologies. Therefore, we propose the development of a database of cooling effectiveness values for a representative collection of cities, seasons, and adaptation measures. The database will provide a framework for planners and practitioners to reliably estimate the cooling impacts of a range of adaptation measures, even if data from the precise city of interest is not available. Planners and practitioners will be able to assess the placed-based cooling impacts of proposed urban cooling strategies prior to deployment, potentially saving considerable resources. It is critical to ensure that appropriate adaptation measures are implemented to meet desired outcomes, rather than utilizing one-size fits all approaches that may not be optimal for a particular location or municipality.

Even with aggressive new laws and ordinances enacted (e.g. Title 24 in California) a uniform deployment of adaptation measures (as simulated here) will take time to be implemented. In many cases, cities will have to choose specific areas or neighborhoods to prioritize for the implementation of adaption measures. While some neighborhoods may receive larger cooling impacts than others, there may be spatial misalignment with populations that are most vulnerable to extreme heat, highlighting the importance of a method that calculates the precise impact of adaptation measures (i.e. ACE) in different urban neighborhoods. This work represents an important first step in the development of universal and broadly applicable metrics of infrastructure-based adaptation effectiveness.

Acknowledgments

This work was supported at Arizona State University by the National Science Foundation Sustainability Research Network (SRN) Cooperative Agreement 1444758 and SES-1520803. ESK was additionally supported by an NSERC Discovery Grant. We acknowledge support from Research Computing at Arizona State University for the provision of high-performance supercomputing services. We would like to thank Judsen Bruzgul (ICF) and Chris Weaver (US Environmental Protection Agency) for helpful comments and feedback. Although the research described in this article has been funded in part by the United States Environmental Protection Agency contract (EP-C-14-001) to ICF, it has not been subject to the Agency's review and therefore does not necessarily reflect the views of the Agency, and no official endorsement should be inferred.

Data availability

The data that support the findings of this study are available from the corresponding author upon reasonable request.

ORCID iDs

Ashley M Broadbent https://orcid.org/0000-0003-1906-8112

References

Ali-Toudert F and Mayer H 2006 Numerical study on the effects of aspect ratio and orientation of an urban street canyon on outdoor thermal comfort in hot and dry climate *Build. Environ.* **41** 94–108

Baklanov A, Molina L T and Gauss M 2016 Megacities, air quality and climate *Atmos. Environ.* **126** 235–49

Bierwagen B G, Theobald D M, Pyke C R, Choate A, Groth P, Thomas J V and Morefield P 2010 National housing and impervious surface scenarios for integrated climate impact assessments *Proc. Natl Acad. Sci.* **107** 20887–92

Bowler D E, Buyung-Ali L, Knight T M and Pullin A S 2010 Urban greening to cool towns and cities: A systematic review of the empirical evidence *Landscape and Urban Planning* **97** 147–55

Broadbent A M, Coutts A M, Tapper N J and Demuzere M 2018a The cooling effect of irrigation on urban microclimate during heatwave conditions *Urban Clim.* **23** 309–29

Broadbent A M, Coutts A M, Tapper N J, Demuzere M and Beringer J 2018b The microscale cooling effects of water

sensitive urban design and irrigation in a suburban environment *Theor. Appl. Climatol.* **134** 1–23
Cao M, Rosado P, Lin Z, Levinson R and Millstein D 2015 Cool Roofs in Guangzhou, China: Outdoor Air Temperature Reductions during Heat Waves and Typical Summer Conditions *Environ. Sci. Tech.* **49** 14672–9
Daniel M, Lemonsu A and Viguié V 2018 Role of watering practices in large-scale urban planning strategies to face the heat-wave risk in future climate *Urban Climate* **23** 287–308
European Centre for Medium-Range Weather Forecasts (ECMWF) ERA-Interim Project 2009 *Research Data Archive at the National Center for Atmospheric Research* Computational and Information Systems Laboratory (accessed 29 November 2016) (https://doi.org/10.5065/D6CR5RD9)
Fallmann J, Emeis S and Suppan P 2013 Mitigation of urban heat stress – a modelling case study for the area of Stuttgart *DIE ERDE – J. Geog. Soc.Berlin* **144** 202–16
Fallmann J, Forkel R and Emeis S 2016 Secondary effects of urban heat island mitigation measures on air quality *Atmos. Environ.* **125** 199–211
Ferrari C, Gholizadeh Touchaei A, Sleiman M, Libbra A, Muscio A, Siligardi C and Akbari H 2014 Effect of aging processes on solar reflectivity of clay roof tiles *Adv. Build. Energy Res.* **8** 28–40
Fouillet A, Rey G, Laurent F, Pavillon G, Bellec S, Guihenneuc-Jouyaux C and Hémon D 2006 Excess mortality related to the August 2003 heat wave in France *Int. Arch. Occup. Environ. Health* **80** 16–24
Georgescu M, Mahalov A and Moustaoui M 2012 Seasonal hydroclimatic impacts of Sun Corridor expansion *Environ. Res. Lett.* **7** 034026
Georgescu M, Morefield P E, Bierwagen B G and Weaver C P 2014 Urban adaptation can roll back warming of emerging megapolitan regions *Proc. Natl Acad. Sci.* **111** 2909–14
Georgescu M, Moustaoui M, Mahalov A and Dudhia J 2013 Summer-time climate impacts of projected megapolitan expansion in Arizona *Nat. Clim. Change* **3** 37
Hirano Y and Fujita T 2012 Evaluation of the impact of the urban heat island on residential and commercial energy consumption in Tokyo *Energy* **37** 371–83
Hondula D M, Balling R C, Vanos J K and Georgescu M 2015 Rising temperatures, human health, and the role of adaptation *Curr. Clim. Change Rep.* **1** 144–54
Huszar P, Halenka T, Belda M, Zak M, Sindelarova K and Miksovsky J 2014 Regional climate model assessment of the urban land-surface forcing over central Europe *Atmos. Chem. Phys.* **14** 12393–413
Krayenhoff E S, Moustaoui M, Broadbent A M, Gupta V and Georgescu M 2018 Diurnal interaction between urban expansion, climate change and adaptation in US cities *Nat. Clim. Change* **8** 1097–103
Krayenhoff E S and Voogt J A 2010 Impacts of urban albedo increase on local air temperature at daily–annual time scales: model results and synthesis of previous work *J. Appl. Meteorol. Climatol.* **49** 1634–48
Levinson R, Berdahl P, Berhe A A and Akbari H 2005 Effects of soiling and cleaning on the reflectance and solar heat gain of a light-colored roofing membrane *Atmos. Environ.* **39** 7807–24
Li D, Bou-Zeid E and Oppenheimer M 2014 The effectiveness of cool and green roofs as urban heat island mitigation strategies *Environ. Res. Lett.* **9** 055002
Li D H, Yang L and Lam J C 2012 Impact of climate change on energy use in the built environment in different climate zones —a review *Energy* **42** 103–12
Li X, Myint S W, Zhang Y, Galletti C, Zhang X and Turner B L 2014 Object-based land-cover classification for metropolitan Phoenix, Arizona, using aerial photography *Int. J. Appl. Earth Obs. Geoinf.* **33** 321–30
Lin S, Fletcher B A, Luo M, Chinery R and Hwang S A 2011 Health impact in New York City during the Northeastern blackout of 2003 *Public Health Rep.* **126** 384–93
Ma H, Shao H and Song J 2013 Modeling the relative roles of the foehn wind and urban expansion in the 2002 Beijing heat wave and possible mitigation by high reflective roofs *Meteorol. Atmos. Phys.* **123** 105–14
Martilli A, Clappier A and Rotach M W 2002 An urban surface exchange parameterisation for mesoscale models *Bound. Layer Meteorol.* **104** 261–304
McEvoy D, Ahmed I and Mullett J 2012 The impact of the 2009 heat wave on Melbourne's critical infrastructure *Local Environ.* **17** 783–96
Miller N L, Hayhoe K, Jin J and Auffhammer M 2008 Climate, extreme heat, and electricity demand in California *J. Appl. Meteorol. Climatol.* **47** 1834–44
Monaghan A J, Steinhoff D F, Bruyere C L and Yates D 2014 *NCAR CESM Global Bias-Corrected CMIP5 Output to Support WRF/MPAS Research* Research Data Archive at the National Center for Atmospheric Research, Computational and Information Systems Laboratory, Boulder, CO
Oleson K W, Bonan G B and Feddema J 2010 Effects of white roofs on urban temperature in a global climate model *Geog. Res. Lett.* **37** L03701
Rizwan A M, Dennis L Y and Chunho L I U 2008 A review on the generation, determination and mitigation of Urban Heat Island *J. Environ. Sci.* **20** 120–8
Salamanca F, Georgescu M, Mahalov A, Moustaoui M and Martilli A 2016 Citywide impacts of cool roof and rooftop solar photovoltaic deployment on near-surface air temperature and cooling energy demand *Bound. Layer Meteorol.* **161** 203–21
Schubert S and Grossman-Clarke S 2013 The influence of green areas and roof albedos on air temperatures during extreme heat events in Berlin, Germany *Meteorologische Zeitschrift* **22** 131–43
Sharma A, Conry P, Fernando H J S, Hamlet A F, Hellmann J J and Chen F 2016 Green and cool roofs to mitigate urban heat island effects in the Chicago metropolitan area: evaluation with a regional climate model *Environ. Res. Lett.* **11** 064004
Skamarock W C and Klemp J B 2008 A time-split nonhydrostatic atmospheric model for weather research and forecasting applications *J. Comput. Phys.* **227** 3465–85
Stewart I D and Oke T R 2012 Local climate zones for urban temperature studies *Bull. Am. Meteorol. Soc.* **93** 1879–900
Stewart I D, Oke T R and Krayenhoff E S 2014 Evaluation of the 'local climate zone' scheme using temperature observations and model simulations *Int. J. Climatol.* **34** 1062–80
Stone B Jr, Vargo J, Liu P, Habeeb D, DeLucia A, Trail M and Russell A 2014 Avoided heat-related mortality through climate adaptation strategies in three US cities *PLoS One* **9** e100852
Taleghani M, Sailor D and Ban-Weiss G A 2016 Micrometeorological simulations to predict the impacts of heat mitigation strategies on pedestrian thermal comfort in a Los Angeles neighborhood *Environ. Res. Lett.* **11** 024003
Thom J K, Coutts A M, Broadbent A M and Tapper N J 2016 The influence of increasing tree cover on mean radiant temperature across a mixed development suburb in Adelaide, Australia *Urban Forestry Urban Greening* **20** 233–42
US EPA 2017 Updates to the demographic and spatial allocation models to produce Integrated Climate and Land Use Scenarios (ICLUS) *Final Report, Version 2* EPA/600/R-16/366F DCUS Environmental Protection Agency, Washington
Vahmani P and Ban-Weiss G A 2016 Impact of remotely sensed albedo and vegetation fraction on simulation of urban climate in WRF-urban canopy model: a case study of the urban heat island in Los Angeles *J. Geophys. Res.: Atmos.* **121** 1511–31
Vahmani P, Sun F, Hall A and Ban-Weiss G 2016 Investigating the climate impacts of urbanization and the potential for cool roofs to counter future climate change in Southern California *Environ. Res. Lett.* **11** 124027
Whitman S, Good G, Donoghue E R, Benbow N, Shou W and Mou S 1997 Mortality in Chicago attributed to the July 1995 heat wave *Am. J. Public Health* **87** 1515–8

Wouters H, De Ridder K, Poelmans L, Willems P, Brouwers J, Hosseinzadehtalaei P and Demuzere M 2017 Heat stress increase under climate change twice as large in cities as in rural areas: a study for a densely populated midlatitude maritime region *Geophys. Res. Lett.* **44** 8997–9007

Wuebbles D J *et al* 2017 *Climate Science Special Report: Fourth National Climate Assessment* Vol 1 (Washington, DC: U.S. Global Change Research Program) pp 35–72

Zhang J, Zhang K, Liu J and Ban-Weiss G 2016 Revisiting the climate impacts of cool roofs around the globe using an Earth system model *Environ. Res. Lett.* **11** 084014